Electric Power Systems Research 189 (2020) 106776

Contents lists available at ScienceDirect

Electric Power Systems Research

journal homepage: www.elsevier.com/locate/epsr

Coordination of Electricity, Heat, and Natural Gas Systems Accounting for Network Flexibility☆

Anna Schwele*[,a], Adriano Arrigo[b], Charlotte Vervaeren[b], Jalal Kazempour[a], François Vallée[b]

[a] Department of Electrical Engineering, Technical University of Denmark, Kgs. Lyngby, Denmark
[b] Electrical Power Engineering Unit, University of Mons, Mons, Belgium

ARTICLE INFO

Keywords:
Combined power-heat-gas dispatch
Convex relaxation
Ex-post feasibility analysis
Multi-energy systems
Second-order cone program

ABSTRACT

Existing energy networks can foster the integration of uncertain and variable renewable energy sources by providing additional operational flexibility. In this direction, we propose a combined power, heat, and natural gas dispatch model to reveal the maximum potential "network flexibility", corresponding to the ability of natural gas and district heating pipelines to store energy. To account for both energy transport and linepack in the pipelines in a computational efficient manner, we explore convex quadratic relaxations of the nonconvex flow dynamics of gas and heat. The resulting model is a mixed-integer second-order cone program. An ex-post analysis ensures feasibility of the heat dispatch, while keeping the relaxation of the gas flow model sufficiently tight. The revealed flexibility is quantified in terms of system cost compared to a dispatch model neglecting the ability of natural gas and district heating networks to store energy.

1. Introduction

Operational flexibility is required to deal with the uncertainty and variability of growing renewable power generation. Flexibility for power systems is often provided by units interfacing other energy sectors, e.g., gas-fired units, combined heat and power (CHP) plants, and heat pumps. These units link the power system with the natural gas and district heating systems, both physically and economically. The gas-fired units usually provide flexibility thanks to their fast-start and ramping capabilities [1]. Similarly, the CHP units can provide flexibility [2], especially extraction CHPs, as they are able to vary their heat to power ratio. Besides, the heat pumps producing heat from electricity can act as power demand side flexibility. The key point is that a strong coordination between power, heat, and natural gas systems is needed to efficiently utilize those existing sources of flexibility. Unlike the power system, in which supply and demand have to be matched instantaneously, there is potential to use the district heating and natural gas networks as energy storage. The district heating and natural gas networks have the ability to store energy in pipelines in the form of time delays of heat propagation and natural gas linepack. This flexibility, the so-called "network flexibility", is provided through the dynamics of energy flow in pipelines, serving as energy storage (known as "virtual storage"). Accounting for these network dynamics can unlock an additional source of flexibility. The existing energy infrastructure in countries with multi-carrier systems, e.g., Denmark, can help mitigate the uncertainty and variability induced by large-scale renewable power penetration.

It is in general a complex task to holistically model the interdependent multi-energy systems while incorporating the energy flow dynamics of each specific energy network. Although there is an extensive literature on integrated energy systems, the majority of previous works either focused on two out of the three (i.e., power, natural gas, and heat) systems, or discarded the network flexibility in heat and natural gas sides, or provided generalized aggregate models, called "energy hubs". With a focus on network flexibility, we first review the existing works addressing the coordination of power and gas systems, then power and heat systems, and finally energy hubs.

The available works in the literature addressing integrated power and natural gas systems model the gas flow dynamics either through partial differential equations [3] or using a reduced version, resulting in a set of nonlinear and nonconvex steady-state equations [4]. These steady-state equations are still complex and cause computational challenges. Therefore, linear approximations [5,6] or quadratic relaxation [7,8] are used to manage the complexity of the natural gas

☆ The work was supported by the Danish EUD Programme through the 'Coordinated Operation of Integrated Energy Systems (CORE)' project under the grant 64017-0005. We thank Lesia Mitridati for her thoughtful discussions and inputs for the heat system model.

* Corresponding author.
E-mail addresses: schwele@elektro.dtu.dk (A. Schwele), adriano.arrigo@umons.ac.be (A. Arrigo), charlotte.vervaeren@umons.ac.be (C. Vervaeren), seykaz@elektro.dtu.dk (J. Kazempour).

https://doi.org/10.1016/j.epsr.2020.106776
Received 28 September 2019; Received in revised form 18 April 2020; Accepted 2 August 2020
Available online 30 August 2020
0378-7796/

flow dynamics, while accounting for the linepack.

In a similar direction, integrated power and heat dispatch models are introduced in Lin et al. [9], Zhou et al. [10], Mitridati and Taylor [11], Li et al. [12], Chen et al. [13]. A proper framework for modeling temperature dynamics in pipelines, time delay of heat transmission, variable supply temperature, and variable mass flow rates will enable exploiting the flexibility from district heating networks. While [9] and [10] consider a constant mass flow rate in pipelines, the heat dispatch models in Mitridati and Taylor [11], Li et al. [12], Chen et al. [13] account for both mass flow rates and inlet temperatures as "control variables", allowing for more degrees of freedom.

The last strand that we explore in the literature is about energy hubs. The concept of energy hubs as a generic aggregate framework for modeling and optimization of multi-energy systems was firstly proposed in Geidl et al. [14]. An energy hub is a unified unit where multiple energy carriers can be converted, conditioned, and stored. However, this generic model fails in accounting for the specific flow dynamics of the energy carriers.

To the best of our knowledge, this is the first work that optimizes the combined dispatch problem for the three energy systems together, accounting for their network and flow dynamics, while dealing with arising nonconvexities. We propose a combined power-heat-gas dispatch that models the interactions of the three energy carriers as well as the network flexibility. As an ideal benchmark, this combined energy dispatch assesses the maximum potential of flexibility that the natural gas and district heating networks can provide for renewable-based power systems. This revealed flexibility is quantified in terms of the reduced operational cost of the entire system compared to a dispatch model neglecting the ability of natural gas and district heating networks to store energy. Since the dynamics of heat and natural gas flow introduce nonconvexities, we explore convex quadratic relaxations of the energy flow model in gas [8,15] and heat [11] systems, including the gas linepack, variable heat temperature and heat mass flow rates as the three degrees of freedom. We recast the original non-convex model as a mixed-integer second-order cone program (MISOCP), and eventually explore the feasibility of solutions achieved.

2. Interactions of Power, Natural Gas, and Heat Systems

Fig. 1 illustrates the interactions among power, heat, and natural gas systems considered in this paper. The dependency of heat and electricity outputs by CHPs and heat pumps induces strong interdependencies between the heat and electricity systems. The heat pumps produce heat from electricity providing electricity demand side flexibility through power-to-heat (P2H). The CHPs produce both electricity and heat from the combustion of a fuel, e.g., biomass or fossil fuels. These synergies physically link the power and heat systems. On the market perspective, the electricity and heat prices are related and determine the profitability and dispatch decision of CHPs and heat pumps. The cost of heat produced by heat pumps depends on electricity prices while the CHP units need to decide both power and heat dispatch with respect to opportunity cost.

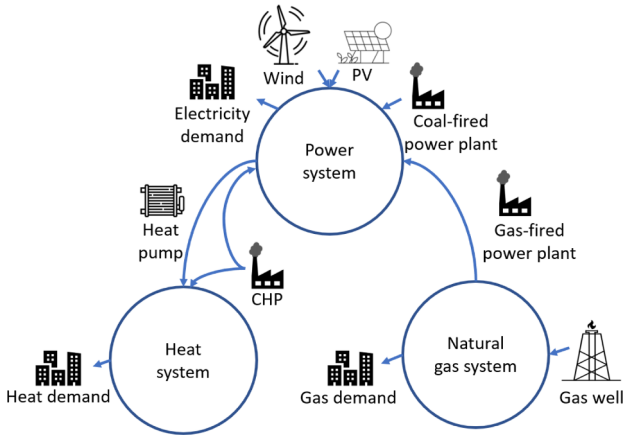

Fig. 1. Interdependent power, natural gas, heat systems.

The gas-fired power plants are usually flexible units that operate at the interface of the power and the natural gas systems, yielding both physical and economic interactions. The gas-fired generators produce electricity from the combustion of natural gas. This conversion is characterized by a conversion factor that accounts for the energy losses. The power output of gas-fired units is directly linked to their fuel consumption. An intermittent dispatch of gas-fired units in the power system and thus gas withdrawal from the gas network brings demand fluctuations and uncertainty into the gas system. Economically, the price of natural gas at which gas-fired units acquire fuel impacts the marginal power production cost of these units, and thus the merit-order in the electricity system.

In addition, there is potential of storing energy in the natural gas and district heating pipelines, which are expected to be even more increased through power-to-gas (P2G) and P2H technologies [16]. This additional source of flexibility from existing infrastructure is explored in the next section.

3. Integrated Multi-Energy Dispatch

This section develops an integrated multi-energy dispatch model, co-optimizing the operation of electricity, heat, and natural gas systems.

3.1. Assumptions

The integrated energy systems assume either a single system operator or a perfect information exchange and timing among the systems. However, in most countries the energy systems are operated independently and sequentially [17]. See [3,18] and [19] for different levels of coordination among energy sectors. The focus of this paper is set on modeling the flexibility provided by the heat and natural gas networks in an efficient manner. Thus, we aim at accurately modeling the heat and gas flow problems and put less attention to the power side by using a simplified lossless DC power flow model. We assume isothermal energy flow in horizontal heat and gas pipelines. We also consider parallel supply and return pipelines for the heating network with both mass flow rates and temperatures as control variables to account for the energy storage capacity in heat pipelines. The natural gas flow is represented by its steady-state gas flow equation. The dynamics in gas pipelines are approximated by accounting for linepack through varying in- and outflows. Compressor stations and water pumps are modeled with a constant factor, while neglecting their fuel and power consumption.

3.2. Objective function

The co-optimization problem aims at minimizing the total cost of operating power, heat, and natural gas systems over time steps t in the planning horizon $\mathcal{T}$. Accordingly, the objective function reads as

$$\min_{\Theta} \sum_{t\in\mathcal{T}} \left(\sum_{i\in C} C_i^{\mathrm{E}}\, p_{i,t} + \sum_{k\in\mathcal{K}} C_k^{\mathrm{G}}\, g_{k,t} + \sum_{i\in\mathcal{HS}} C_i^{\mathrm{H}}\, Q_{i,t} + \sum_{i\in\mathcal{CHP}} C_i(\rho_i^{\mathrm{E}}\, p_{i,t} + \rho_i^{\mathrm{H}}\, Q_{i,t}) \right), \tag{1a}$$

where the set of decision variables is $\Theta = \{p_{i,t}, w_{j,\,t}, \theta_{n,t}, f_{n,r,t}, q_{m,u,t}, q^{\mathrm{in}}_{m,u,t}, q^{\mathrm{out}}_{m,u,t}, h_{m,u,t}, pr_{m,t}, g_{k,t}, Q_{i,t}, pr^{\mathrm{S}}_{o,t}, pr^{\mathrm{R}}_{o,t}, mf^{\mathrm{HES}}_{o,t}, mf^{\mathrm{HS}}_{i,t}, mf^{\mathrm{S}}_{o,v,t}, mf^{\mathrm{R}}_{o,v,t}, T^{\mathrm{S}}_{o,t}, T^{\mathrm{R}}_{o,t}, T^{\mathrm{S,in}}_{o,v,t}, T^{\mathrm{R,in}}_{o,v,t}, T^{\mathrm{S,out}}_{o,v,t}, T^{\mathrm{R,out}}_{o,v,t}, \tau^{\mathrm{S}}_{o,v,t}, \tau^{\mathrm{R}}_{o,v,t}, u^{\mathrm{S}}_{o,v,\eta,t}, u^{\mathrm{R}}_{o,v,\eta,t}\}$. The first term of (1a) represents the operating cost of non-gas fired units $i \in C$ given marginal

cost parameters C_i^{E} and power production $p_{i,t}$. The second term corresponds to the cost of gas suppliers $k \in \mathcal{K}$ with marginal gas supply cost parameters C_i^{G} and gas supply $g_{k,t}$. The third term refers to the operating cost of heat boilers $i \in \mathcal{HS}$ given marginal cost parameters C_i^{H} and heat production $Q_{i,t}$. The last term models the operating cost of CHPs $i \in \mathcal{CHP}$ as a linear function of marginal cost C_i, electricity and heat fuel efficiency ρ_i^{E} and ρ_i^{H}, and the respective power and heat production level.

The objective function (1a) is subject to power constraints (2), heat constraints (3), natural gas constraints (4), as well as constraints (5) which couple the three systems. All these constraints are described in the following.

3.3. Power system constraints

The power system constraints taking into account a lossless DC power flow model are

$$0 \le p_{i,t} \le \overline{p}_i, \forall\, i, t, \tag{2a}$$

$$0 \le w_{j,t} \le \overline{w}_{j,t}, \forall\, j, t, \tag{2b}$$

$$f_{n,r,t} = B_{n,r}(\theta_{n,t} - \theta_{r,t}), \forall\, (n, r) \in \mathcal{L}, t, \tag{2c}$$

$$-\overline{f}_{n,r} \le f_{n,r,t} \le \overline{f}_{n,r}, \forall\, (n, r) \in \mathcal{L}, t, \tag{2d}$$

$$-\pi \le \theta_{n,t} \le \pi, \forall\, n, t, \quad \theta_{n,t} = 0, \forall\, n{:}\, ref, t, \tag{2e}$$

where parameters $\overline{p}_i$ and $\overline{w}_{j,t}$ in (2a) and (2b) restrict the power production $p_{i,t}$ and $w_{j,\,t}$ of conventional generators $i \in \mathcal{I}$ and renewable generators $j \in \mathcal{J}$, respectively. Constraints (2c) define the power flow $f_{n,r,t}$ along transmission line (n, r) by line susceptance $B_{n,r}$ and voltage angles $\theta_{n,t}$ at adjacent nodes n and r. The power flow is restricted to transmission line limits $\overline{f}_{n,r}$ by (2d). Constraints (2e) limit the voltage angles, and set the voltage angle to zero at the reference node.

3.4. Heat system constraints

Following [11], the heat dispatch model considers both mass flow rates and inlet temperatures as control variables, accounting for temperature dynamics and time delays as

$$D_{o,t}^{\mathrm{H}} = c\; mf_{o,t}^{\mathrm{HES}}(T_{o,t}^{\mathrm{S}} - T_{o,t}^{\mathrm{R}}), \forall\, o, t, \tag{3a}$$

$$Q_{i,t} = c\; mf_{i,t}^{\mathrm{HS}}(T_{o,t}^{S} - T_{o,t}^{\mathrm{R}}), \forall\, o, i \in \mathcal{A}_o^{\mathrm{HS}}, t, \tag{3b}$$

$$0 \le Q_{i,t} \le \overline{Q}_i, \forall\, i \in \mathcal{HS}, t, \tag{3c}$$

$$\underline{pr}_o^{\mathrm{HES}} \le pr_{o,t}^{\mathrm{S}} - pr_{o,t}^{\mathrm{R}}, \forall\, o, t, \tag{3d}$$

$$\underline{mf}_o^{\mathrm{HES}} \le mf_{o,t}^{\mathrm{HES}} \le \overline{mf}_o^{\mathrm{HES}}, \forall\, o, t, \tag{3e}$$

$$\underline{mf}_i^{\mathrm{HS}} \le mf_{i,t}^{\mathrm{HS}} \le \overline{mf}_i^{\mathrm{HS}}, \forall\, i \in \mathcal{HS}, t, \tag{3f}$$

$$\underline{mf}_{o,v}^{\mathrm{S}} \le mf_{o,v,t}^{\mathrm{S}} \le \overline{mf}_{o,v}^{\mathrm{S}}, \forall\, (o, v) \in \mathcal{P}, t, \tag{3g}$$

$$\underline{mf}_{o,v}^{\mathrm{R}} \le mf_{o,v,t}^{\mathrm{R}} \le \overline{mf}_{o,v}^{\mathrm{R}}, \forall\, (o, v) \in \mathcal{P}, t, \tag{3h}$$

$$\sum_{v:(o,v)\in\mathcal{P}} mf_{v,o,t}^{\mathrm{S}} + \sum_{i\in\mathcal{A}_o^{\mathrm{HS}}} mf_{i,t}^{\mathrm{HS}} = \sum_{v:(o,v)\in\mathcal{P}} mf_{o,v,t}^{\mathrm{S}} + mf_{o,t}^{\mathrm{HES}}, \forall\, o, t, \tag{3i}$$

$$\sum_{v:(o,v)\in\mathcal{P}} mf_{v,o,t}^{\mathrm{R}} + \sum_{i\in\mathcal{A}_o^{\mathrm{HS}}} mf_{i,t}^{\mathrm{HS}} = \sum_{v:(o,v)\in\mathcal{P}} mf_{o,v,t}^{\mathrm{R}} + mf_{o,t}^{\mathrm{HES}}, \forall\, o, t, \tag{3j}$$

$$L_{o,v}(mf_{o,v,t}^{\mathrm{S}})^2 = pr_{o,t}^{\mathrm{S}} - pr_{v,t}^{\mathrm{S}}, \forall\, (o, v) \in \mathcal{P}, t, \tag{3k}$$

$$L_{o,v}(mf_{o,v,t}^{\mathrm{R}})^2 = pr_{v,t}^{\mathrm{R}} - pr_{o,t}^{\mathrm{R}}, \forall\, (o, v) \in \mathcal{P}, t, \tag{3l}$$

$$\underline{pr}_o^{\mathrm{S}} \le pr_{o,t}^{\mathrm{S}} \le \overline{pr}_o^{\mathrm{S}}, \quad \underline{pr}_o^{\mathrm{R}} \le pr_{o,t}^{\mathrm{R}} \le \overline{pr}_o^{\mathrm{R}}, \forall\, o, t, \tag{3m}$$

$$\underline{T}_o^{\mathrm{S}} \le T_{o,t}^{\mathrm{S}} \le \overline{T}_o^{\mathrm{S}}, \quad \underline{T}_o^{\mathrm{R}} \le T_o^{\mathrm{R}} \le \overline{R}_o^{\mathrm{S}}, \forall\, o, t, \tag{3n}$$

$$T_{o,v,t}^{\mathrm{S,in}} = T_{o,t}^{\mathrm{S}}, \quad T_{o,v,t}^{\mathrm{R,in}} = T_{v,t}^{\mathrm{R}}, \quad \forall\, (o, v) \in \mathcal{P}, t, \tag{3o}$$

$$T_{v,t}^{\mathrm{S}} = T_{o,v,t}^{\mathrm{S,out}}, \quad T_{o,t}^{\mathrm{R}} = T_{o,v,t}^{\mathrm{R,out}}, \forall\, (o, v) \in \mathcal{P}, t, \tag{3p}$$

$$T_{o,v,t}^{\mathrm{S,out}} = T_{o,v,(t-\tau)}^{\mathrm{S,in}}\left(1 - \frac{2\mu_{o,v}}{c\rho R_{o,v}}\tau_{o,v,t}^{\mathrm{S}}\right), \forall\, (o, v) \in \mathcal{P}, t, \tag{3q}$$

$$T_{o,v,t}^{\mathrm{R,out}} = T_{o,v,(t-\tau)}^{\mathrm{R,in}}\left(1 - \frac{2\mu_{o,v}}{c\rho R_{o,v}}\tau_{o,v,t}^{\mathrm{R}}\right), \forall\, (o, v) \in \mathcal{P}, t, \tag{3r}$$

$$M(u_{o,v,\eta,t}^{\mathrm{S}} - 1) \le \sum_{\tilde{\eta}=t-\eta}^{t} \frac{mf_{o,v,\tilde{\eta}}^{\mathrm{S}}}{\pi R_{o,v}^2 \rho}\Delta t - L_{o,v} \le M\; u_{o,v,\eta,t}^{\mathrm{S}},$$
$$\forall\, (o, v) \in \mathcal{P}, \eta \in \{0, \ldots, \overline{\tau}_{o,v}^{\mathrm{S}}\}, t, \tag{3s}$$

$$M(u_{o,v,\eta,t}^{\mathrm{R}} - 1) \le \sum_{\tilde{\eta}=t-\eta}^{t} \frac{mf_{o,v,\tilde{\eta}}^{\mathrm{R}}}{\pi R_{o,v}^2 \rho}\Delta t - L_{o,v} \le M\; u_{o,v,\eta,t}^{\mathrm{R}},$$
$$\forall\, (o, v) \in \mathcal{P}, \eta \in \{0, \ldots, \overline{\tau}_{o,v}^{\mathrm{R}}\}, t, \tag{3t}$$

$$\tau_{o,v,t}^{\mathrm{S}} = \sum_{\eta=1}^{\overline{\tau}_{o,v}^{\mathrm{S}}} \eta(u_{o,v,\eta,t}^{\mathrm{S}} - u_{o,v,(\eta-1),t}^{\mathrm{S}}), \forall\, (o, v) \in \mathcal{P}, t, \tag{3u}$$

$$\tau_{o,v,t}^{\mathrm{R}} = \sum_{\eta=1}^{\overline{\tau}_{o,v}^{\mathrm{R}}} \eta(u_{o,v,\eta,t}^{\mathrm{R}} - u_{o,v,(\eta-1),t}^{\mathrm{R}}), \forall\, (o, v) \in \mathcal{P}, t. \tag{3v}$$

In (3a), the inelastic heat demand $D_{o,t}^{\mathrm{H}}$ in each district heating node o is related to the specific heat capacity of water c, heat exchanger mass flows $mf_{o,t}^{\mathrm{HES}}$ and temperatures at node o of both supply $T_{o,t}^{\mathrm{S}}$ and return network $T_{o,t}^{\mathrm{R}}$. Constraints (3b) relate heat production $Q_{i,t}$, which is limited by its capacity $\overline{Q}_i$ in (3c), to heat station mass flows $mf_{i,t}^{\mathrm{HS}}$ and temperature gradients between supply and return networks at heat stations $i \in \mathcal{A}_o^{\mathrm{HS}}$ located at node o. The minimum pressure gradient $\underline{pr}_o^{\mathrm{HES}}$ between the pressures $pr_{o,t}^{\mathrm{S}}$ and $pr_{o,t}^{\mathrm{R}}$ between supply and return network at heat exchanger station node o is enforced by (3d). The mass flows are restricted in (3e)–(3h) at heat exchange stations by lower bound $\underline{mf}_o^{\mathrm{HES}}$ and upper bound $\overline{mf}_o^{\mathrm{HES}}$, at heat stations $i \in \mathcal{HS}$ by $\underline{mf}_i^{\mathrm{HS}}$ and $\overline{mf}_i^{\mathrm{HS}}$, and supply and return pipelines $(o, v) \in \mathcal{P}$ by $\underline{mf}_{o,v}^{\mathrm{S/R}}$ and $\overline{mf}_{o,v}^{\mathrm{S/R}}$, respectively. Constraints (3i) and (3j) balance mass flow for supply and return network nodes. The Darcy-Weisbach Eqs. (3k) and (3l) relate pressure losses due to friction inside the supply and return pipelines to mass flow rates via pressure loss coefficient $L_{o,\,v}$. Constraints (3m) and (3n) put upper and lower bounds on nodal pressure ($\underline{pr}_o^{\mathrm{S/R}}$, $\overline{pr}_o^{\mathrm{S/R}}$,) and temperature ($\underline{T}_o^{\mathrm{S/R}}$, $\overline{T}_o^{\mathrm{S/R}}$) in both supply and return networks. Pursuing further clarity, the concept of heat flows in these parallel pipelines is shown in Fig. 2.

The temperature at the entrance of the pipe $T_{o,v,t}^{\mathrm{S/R,in}}$ is defined in (3o). Temperature mixing is given by outlet temperatures $T_{o,v,t}^{\mathrm{S/R,out}}$ in (3p). The heat losses are approximated using first-order Taylor series expansion of the heat propagation Eqs. (3q) and (3r) for supply and return

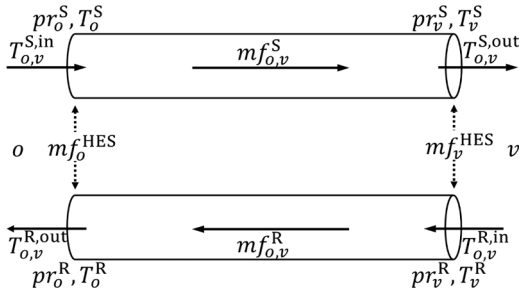

Fig. 2. Heat flow in parallel supply and return pipeline (time index t is dropped for notational clarity).

pipelines, respectively. The water temperatures at the outlet of a pipe $T^{\mathrm{S/R,out}}_{o,v,t}$ corresponds to past temperatures at the inlet $T^{\mathrm{S/R,in}}_{o,v,(t-\tau)}$ at previous time $t-\tau$ minus heat losses in the pipe. These losses are given by thermal loss coefficient $\mu_{o,v}$, specific water capacity c, water density ρ and the radius of the pipe $R_{o,v}$. We introduce auxiliary binary variables $u^{\mathrm{S/R}}_{o,v,\eta,t} \in \{0, 1\}$ and the sufficiently large positive constant M to help define the varying time delays $\tau^{\mathrm{S/R}}_{o,v,t}$. The delay of heat propagation depends on the mass flow rate at each time step and for each pipe and the length of the pipe and is defined by (3s) and (3t). Finally, (3u) and (3v) ensure the minimum delay with the maximum time delay parameters $\overline{\tau}^{\mathrm{S/R}}_{o,v}$, depending on the physical characteristics of the pipelines.

3.5. Natural gas system constraints

Similar to the models in Schwele et al. [7] and Chen et al. [8], we dispatch the natural gas system using a steady-state natural gas flow model accounting for linepack in the pipelines. The constraints are

$$0 \le g_{k,t} \le \overline{g}_k, \forall\, k, t, \tag{4a}$$

$$\underline{pr}_m \le pr_{m,t} \le \overline{pr}_m, \forall\, m, t, \tag{4b}$$

$$pr_{u,t} \le \Gamma_{m,u}\, pr_{m,t}, \forall\, (m,u) \in \mathcal{Z}, t, \tag{4c}$$

$$q_{m,u,t} = K_{m,u}\sqrt{pr^2_{m,t} - pr^2_{u,t}}, \forall\, (m,u) \in \mathcal{Z}, t, \tag{4d}$$

$$q_{m,u,t} = \frac{q^{\mathrm{in}}_{m,u,t} + q^{\mathrm{out}}_{m,u,t}}{2}, \forall\, (m,u) \in \mathcal{Z}, t, \tag{4e}$$

$$h_{m,u,t} = S_{m,u}\frac{pr_{m,t} + pr_{u,t}}{2}, \forall\, (m,u) \in \mathcal{Z}, t, \tag{4f}$$

$$h_{m,u,t} = h_{m,u,(t-1)} + q^{\mathrm{in}}_{m,u,t} - q^{\mathrm{out}}_{m,u,t}, \forall\, (m,u) \in \mathcal{Z}, t > 1, \tag{4g}$$

$$h_{m,u,t} = H^0_{m,u} + q^{\mathrm{in}}_{m,u,t} - q^{\mathrm{out}}_{m,u,t}, \forall\, (m,u) \in \mathcal{Z}, t = 1, \tag{4h}$$

$$H^0_{m,u} \le h_{m,u,t}, \forall\, (m,u) \in \mathcal{Z}, t = |\mathcal{T}|, \tag{4i}$$

where (4a) enforces the capacity $\overline{g}_k$ for gas supply $g_{k,t}$, whereas (4b) imposes the upper and lower limits $\underline{pr}_m$ and $\overline{pr}_m$ for pressure $pr_{m,t}$ at each gas node m. Constraints (4c) provide a linearized representation of compressor stations along pipeline $(m,u) \in \mathcal{Z}$ with fixed compression ratio $\Gamma_{m,u}$. The non-negative natural gas flow $q_{m,u,t} \ge 0$ from node m to u is defined by the Weymouth Eq. (4d). This equation relates the flow along a pipeline to the difference of squared pressures at beginning node m and ending node u of the pipeline and Weymouth constant $K_{m,u}$. We define this natural gas flow along a pipe as the average of inflows $q^{\mathrm{in}}_{m,u,t}$ into a pipeline and outflows $q^{\mathrm{out}}_{m,u,t}$ out of each pipeline in (4e), see Fig. 3. Constraints (4f) define linepack $h_{m,u,t}$ as a function of pressures at both ends of the pipeline and pipeline characteristics $S_{m,u}$. Constraints (4g) balance in- and outflows with linepack storage in pipelines. Initial linepack $H^0_{m,u}$ at the beginning of the planning horizon and minimum linepack level in the final time period of the optimization horizon are ensured by (4h) and (4i) to avoid depletion of natural gas in the network.

3.6. Coupling constraints

The units at the interface, i.e., CHPs, heat pumps, and gas-fired generators, link the three systems, see Fig. 1. The following coupling constraints describe the interdependencies among the energy carriers and how the units at the interfaces link the systems linearly:

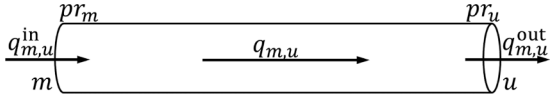

Fig. 3. Natural gas flow along a pipeline (time index t is removed).

$$\sum_{k\in\mathcal{A}^{\mathrm{K}}_m} g_{k,t} - \sum_{i\in\mathcal{A}^{\mathrm{G}}_m} \phi_i\, p_{i,t} - \sum_{u:(m,u)\in\mathcal{Z}} (q^{\mathrm{in}}_{m,u,t} - q^{\mathrm{out}}_{u,m,t}) = D^{\mathrm{G}}_{m,t}, \forall\, m, t, \tag{5a}$$

$$r_i Q_{i,t} \le p_{i,t}, \forall\, i \in \mathcal{CHP}, t, \tag{5b}$$

$$0 \le \rho^{\mathrm{E}}_i p_{i,t} + \rho^{\mathrm{H}}_i Q_{i,t} \le \overline{p}_i, \forall\, i \in \mathcal{CHP}, t, \tag{5c}$$

$$Q_{i,t} = COP_i D^{\mathrm{HP}}_{i,t}, \forall\, i \in \mathcal{HP}, t, \tag{5d}$$

$$\sum_{i\in\mathcal{A}^{\mathrm{I}}_n} p_{i,t} + \sum_{j\in\mathcal{A}^{\mathrm{J}}_n} w_{j,t} - \sum_{r:(n,r)\in\mathcal{L}} f_{n,r,t} = D^{\mathrm{E}}_{n,t} + \sum_{i\in\mathcal{A}^{\mathrm{HP}}_n} D^{\mathrm{HP}}_{i,t}, \forall\, n, t. \tag{5e}$$

Constraints (5a) balance gas injection and inelastic demand $D^{\mathrm{G}}_{m,t}$ of units $\mathcal{A}^{(\cdot)}_m$ located at node m with in- and outflow from and to adjacent nodes u of the natural gas network. The fuel consumption of natural gas-fired generators is translated into a nodal, time-varying gas demand $\phi_i p_{i,t}$ via fuel conversion factor ϕ_i. Constraints (5b) and (5c) define the joint feasible operating region of an extraction CHP. The heat and electricity outputs $Q_{i,t}$ and $p_{i,t}$ of each CHP are linked through output ratio r_i in (5b). The total capacity limits of CHP units are enforced by (5c). Constraints (5d) translate the heat production of heat pumps $Q_{i,t}$ to power consumption $D^{\mathrm{HP}}_{i,t}$ by the coefficient of performance COP_i. Nodal power balance (5e) matches the inelastic electricity demand $D^{\mathrm{E}}_{n,t}$ and electricity consumption by heat pumps $D^{\mathrm{HP}}_{i,t}$ with the power generation from conventional, gas-fired, CHP and renewable units $\mathcal{A}^{(\cdot)}_n$ located at node n accounting for power flows along adjacent power transmission lines.

The resulting model (1)-(5) is a mixed-integer non-linear program (MINLP). It is a challenging problem to deal with, as there is no off-the-shelf solver available for a MINLP problem. In the next section, while keeping the binary variables, we convexify the nonlinearities arising from heat and gas flow models. This will eventually result in a MISOCP.

4. Convexification

The non-convexities of MINLP model (1)–(5) arise from quadratic equality constraints (3k), (3l), and (4d), as well as bilinear terms in (3a), (3b), (3q), and (3r). We first apply quadratic relaxations that allow for modeling both natural gas flow and heat mass flow related to pressure drops. Then, bilinear terms are convexified using a linearization technique [11] and McCormick relaxations [20].

4.1. Quadratic relaxation

The steady-state gas flow Eq. (4d) can be made convex using a second-order cone (SOC) relaxation. We first reformulate (4d) as

$$q^2_{m,u,t} \le K^2_{m,u}(pr^2_{m,t} - pr^2_{u,t}), \forall\, (m,u) \in \mathcal{Z}, t, \tag{6a}$$

$$q^2_{m,u,t} \ge K^2_{m,u}(pr^2_{m,t} - pr^2_{u,t}), \forall\, (m,u) \in \mathcal{Z}, t, \tag{6b}$$

and then drop (6b). Now, (6a) is a SOC constraint, see left plot in Fig. 4. Reference [21] proves the SOC relaxation to be exact under several conditions. The pressure loss Eqs. (3k) and (3l) can be convexified in a similar manner. After reformulating them as

$$L_{o,v}(mf^{\mathrm{S/R}}_{o,v,t})^2 \le pr^{\mathrm{S/R}}_{v,t} - pr^{\mathrm{S/R}}_{o,t}, \forall\, (o,v) \in \mathcal{P}, t, \tag{7a}$$

$$L_{o,v}(mf^{\mathrm{S/R}}_{o,v,t})^2 \ge pr^{\mathrm{S/R}}_{v,t} - pr^{\mathrm{S/R}}_{o,t}, \forall\, (o,v) \in \mathcal{P}, t, \tag{7b}$$

and dropping (7b), the remaining (7a) are SOC constraints, as shown in the middle plot of Fig. 4.

4.2. Linearization and relaxation of bilinear terms

4.2.1. Linearization

The heat propagation Eqs. (3q) and (3r) are non-convex due to the bilinear terms $T^{\mathrm{S/R,in}}_{o,v,(t-\tau^{\mathrm{S/R}}_{o,v,t})}\tau^{\mathrm{S/R}}_{o,v,t}$ and the use of varying time delays $\tau^{\mathrm{S/R}}_{o,v,t}$ as

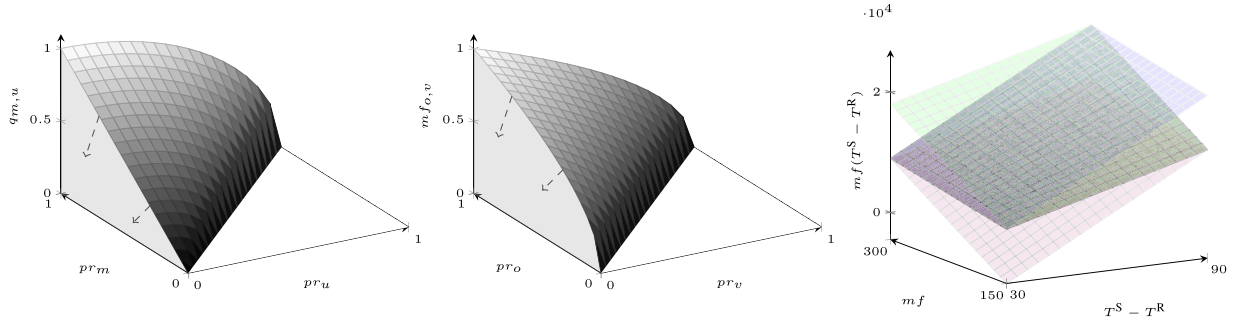

Fig. 4. Three dimensional illustrations of the relaxations. The plots on the left-hand, middle, and right-hand sides show the relaxation corresponding to constraints (6a), (7a), and (3a) and (3b), respectively. The left-hand plot shows the relaxed Weymouth Eq. (6a) for flow $q_{m,u}$ as a function of pressures at inlet and outlet nodes, i.e., pr_m and pr_u. In the middle, the relaxation of the Darcy-Weisbach Eq. (7a) is plotted with mass flow $mf_{o,v}$ as a function of pressures at inlet and outlet nodes, i.e., pr_o and pr_v. The dashed arrows in the left and middle plots show the area under the surface added to the feasible space by conic relaxation. McCormick envelopes for bilinear terms $mf\,(T^S - T^R)$ are illustrated in the right-hand plot. Time index t is dropped for notational clarity.

indices. We follow the approach in Mitridati and Taylor [11] to linearize these constraints in an exact way using auxiliary binary variables $v^{S/R}_{o,v,\eta,t} \in \{0, 1\}$ as well as a sufficiently large positive constant M. Pursuing linearity of (3q), we include the following constraints:

$$-M\, v^{S}_{o,v,\eta,t} \le \tilde{T}^{S,in}_{o,v,\eta,t} \le M\, v^{S}_{o,v,\eta,t}, \quad \forall\, (o,v) \in \mathcal{P},\, \eta \in \{0,\dots,\bar{\tau}^{S}_{o,v}\},\, t, \tag{8a}$$

$$M\,(v^{S}_{o,v,\eta,t} - 1) \le \tilde{T}^{S,in}_{o,v,\eta,t} - \tilde{T}^{S,in}_{o,v,(t-\eta)}\left(1 - \frac{2\mu_{o,v}}{c\rho R_{o,v}}\eta\right) \le M(1 - v^{S}_{o,v,\eta,t}),\ \forall\, (o,v) \in \mathcal{P},\, \eta \in \{0,\dots,\bar{\tau}^{S}_{o,v}\},\, t, \tag{8b}$$

$$M\,(v^{S}_{o,v,\eta,t} - 1) \le \eta - \tau^{S}_{o,v,t} \le M(1 - v^{S}_{o,v,\eta,t}),\ \forall\, (o,v) \in \mathcal{P},\, \eta \in \{0,\dots,\bar{\tau}^{S}_{o,v}\},\, t, \tag{8c}$$

$$\sum_{\eta=0}^{\bar{\tau}^{S}} v^{S}_{o,v,\eta,t} = 1,\ \forall\, (o,v) \in \mathcal{P},\, t, \tag{8d}$$

$$T^{S,out}_{o,v,t} = \sum_{\eta=0}^{\bar{\tau}^{S}_{o,v}} \tilde{T}^{S,in}_{o,v,\eta,t},\ \forall\, (o,v) \in \mathcal{P},\, t. \tag{8e}$$

Note that (3r) can be reformulated in the same manner.

4.2.2. McCormick relaxation

Pursuing convexity, bilinear terms $mf\,(T^S - T^R)$ in (3a) and (3b) are linearized using McCormick envelopes [20], illustrated in the right plot of Fig. 4. We can now solve (1)–(3p), (3s)–(4c), (4e)–(5), (6a), (7a), (8) as a MISOCP.

5. Case Study

5.1. Input data

We apply the proposed combined power-heat-gas dispatch (1)–(5) with convexified formulation from Section 4 on an integrated energy model based on the IEEE 24-bus reliability test system [22], coupled with a 12-node gas network [5] and a 3-node district heating network [11] over a 24-hour scheduling horizon. This integrated energy system is depicted in Fig. 5. All input data can be found in the online appendix [23].

A wind farm, whose power output realization is given in Fig. 6, five non-gas-fired units, six gas-fired units and a biomass-fueled CHP unit are available to supply electricity load. The CHP unit and a heat pump cover the heat demand, while gas fuel is provided by three gas suppliers. The electricity, heat and natural gas loads are shown in Fig. 6.

The optimization problem is solved on an Intel core i5 computer clocking at 2.3 GHz, using Gurobi solver 8.0 with Python, allowing the instance to reach an optimality gap of 0.02% in less than one second.

5.2. Numerical results

We first provide the results obtained for the total operational cost of the integrated energy system, i.e., the optimal value of objective function (1a). This cost is achieved under varying levels of wind power penetration, which is defined as the ratio of total wind power capacity to maximum electricity demand. Fig. 7 shows decreasing operational cost of the integrated energy system for increasing levels of wind power penetration. We compare these results to a dispatch that does not account for network flexibility. We replace gas linepack constraints (4f)–(4i) by $q^{in}_{m,u,t} = q^{out}_{m,u,t}$, $\forall\, (m,u) \in \mathcal{Z},\, t$, balancing in- and outflow of gas pipelines neglecting the linepack. The flexibility from the heating network given in constraints (3) is omitted by dispatching heat according to heat production capacity limits (3c) and system-wide heat balance $\sum_{i\in\mathcal{HES}} D^{H}_{i,t} = \sum_{i\in\mathcal{HS}} Q_{i,t},\, \forall\, t$. Accounting for flow dynamics and storage in gas and heat pipelines decreases the total system cost by 2% on average compared with the case neglecting network flexibility.

Fig. 8 shows the total amount of natural gas and heat supplied and consumed for the entire 24-hour horizon. When modeling linepack, consumption and supply of natural gas and heat do not necessarily need to be matched in each time period. The amount of energy stored in the pipelines (which is highlighted in shaded zones in Fig. 8) directly impacts the profiles of natural gas and heat supply. When the wind power generation is high in the beginning hours of the time horizon, heat is produced by heat pumps and stored in the district heating system in the first seven hours. Simultaneously, natural gas is accumulated within pipelines until hour 11. During a period of low output from wind power and high power and heat demand in hours 19–23, the linepack stored in gas pipelines is used to fuel electricity production and heat that was previously stored in the district heating network is consumed.

The flexibility provided by energy storage in the networks allows not only to decouple gas supply from consumption and heat production from demand, but also shifting electricity production and consumption. Network flexibility improves utilization of power production from variable renewable sources. This is evident in reduced wind curtailment over the planning horizon. As shown in Fig. 9, the wind curtailment is reduced by 1.2% on average when accounting for energy storage in networks.

5.3. Feasibility verification

Relaxing the original MINLP into a MISOCP enables us to efficiently find an optimal solution. However, this solution is based on relaxations of the original constraints, and therefore, the original constraints might not be hold. Thus, an ex-post evaluation of the results obtained from the MISOCP with respect to the original set of constraints is required.

First, we check the feasibility of results for the heat system. We fix

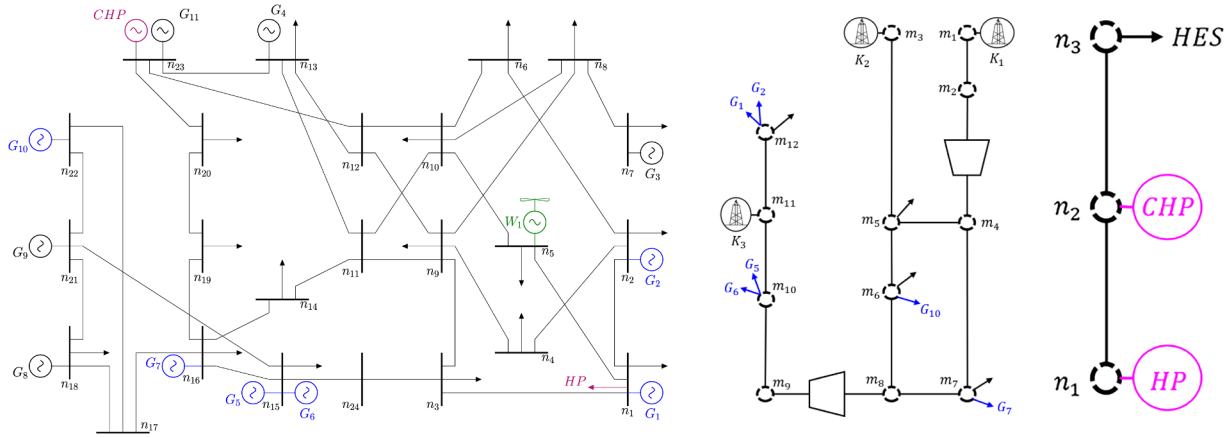

Fig. 5. Illustration of the integrated energy system for the case study. The graphs on the left-hand, middle, and right-hand sides show the topologies corresponding to power, natural gas, and heat networks, respectively. The left-hand plot shows the IEEE 24-bus reliability test system layout. In the middle, the 12-node natural gas network is plotted. The 3-bus heat network is illustrated in the right-hand plot.

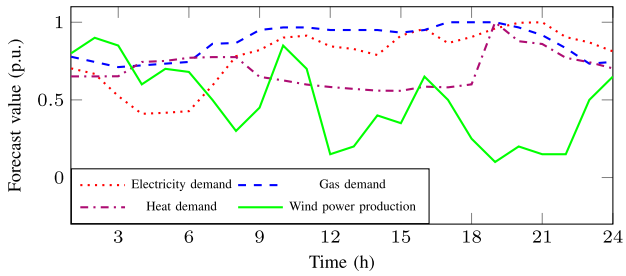

Fig. 6. The hourly inelastic electricity, heat, and gas loads as well as the hourly deterministic wind power forecast, all in per-unit.

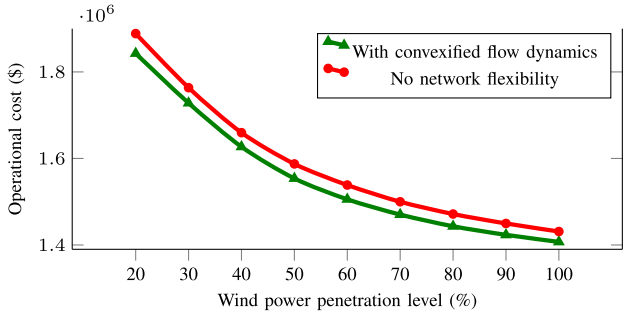

Fig. 7. Total operational cost of the entire integrated energy system in cases with and without considering network flexibility as a function of wind power penetration, i.e., the total wind power capacity divided by the maximum power demand.

all mass flow rates and binary variables to the optimal value obtained from the MISCOP. We then solve the original set of constraints resulting in a linear set of equations to obtain new values for pressures and temperatures at heat nodes. To solve the resulting system of equations, we adjust the nodal temperature bounds, which results in about 1% increase of the temperature interval. We recover a feasible solution for the real equations of the heat network under this slight parametric change.

Then, we check the feasibility of solution achieved for the natural gas system. We compute the normalized root mean square error (NRMSE), where the error is defined as the difference between the left-hand and right-hand sides of the relaxed Weymouth Eq. (6a) for all time steps and pipelines. The average NRMSE for the different wind power penetrations is 1.84%. We observe that there is no mismatch in most pipelines and time steps, but it reaches 100% in pipelines 3, 7 and 8 during particular periods, see Fig. 10. Note that the pipelines in the

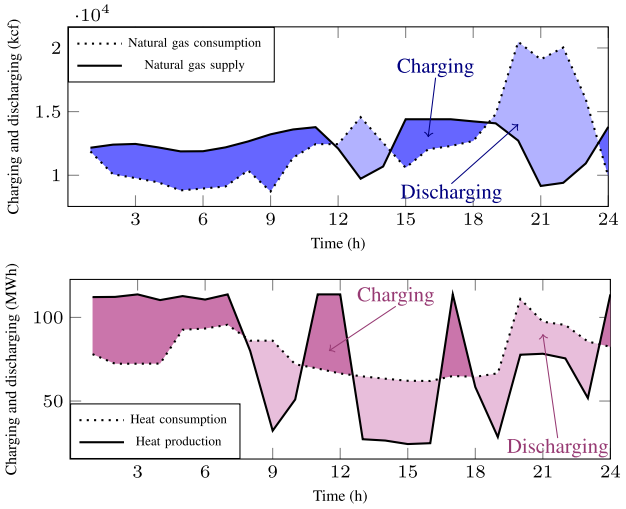

Fig. 8. The hourly profiles of natural gas (upper plot) and heat (lower plot) systems, illustrating the hourly total supply, total consumption, and the charging/discharging energy by network.

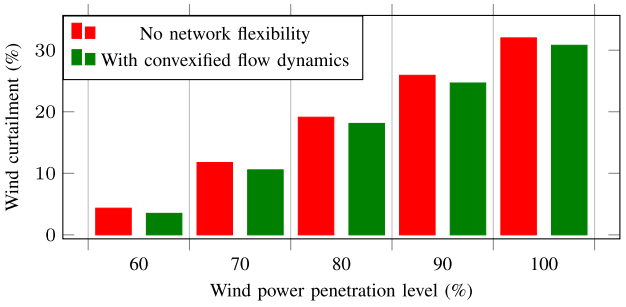

Fig. 9. Comparison of wind curtailment with and without considering network flexibility of natural gas and heat systems.

network loop are prone to mismatch. Since the occurrence rate of error is low, the relaxation seems sufficiently tight.

6. Conclusion

We introduced an integrated power-heat-gas dispatch accounting for the interactions of the three energy carriers and flow dynamics in an efficient manner using convex relaxations. This ideal benchmark showed the maximum potential of flexibility provided by the existing

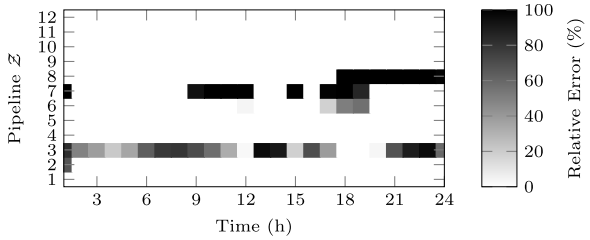

Fig. 10. Matrix plot of the relative error between right-hand and left-hand sides of relaxed Weymouth Eq. (6a) for each time step (x-axis) and each pipeline (y-axis).

natural gas and heating infrastructure. We quantified the social value in terms of reduced total system cost that short-term operational flexibility from energy storage in district heating and natural gas networks can provide for the power system. This coordination of energy carriers is an inexpensive solution for increasing the flexibility of the system compared to investing in other storage options and grid reinforcement and interconnections.

As future works, it is of interest to explore the additional alternatives to further tighten the relaxation techniques used. It is also of interest to investigate how the natural gas and heat networks can provide the flexibility without need to solve a co-optimization, and how this flexibility should be monetized and paid. Furthermore, increasing the interactions among all systems, e.g., gas-fueled CHPs, P2G units, natural gas boilers, and multi-generation units, in a larger test case is left for future research.

Declaration of Competing Interest

The authors declare that they have no known competing financial interests or personal relationships that could have appeared to influence the work reported in this paper.

References

[1] E. Litvinov, F. Zhao, T. Zheng, Electricity markets in the United States: Power industry restructuring processes for the present and future, IEEE Power Energy Mag. 17 (1) (2019) 32–42.
[2] X. Chen, C. Kang, M. O'Malley, Q. Xia, J. Bai, C. Liu, R. Sun, W. Wang, H. Li, Increasing the flexibility of combined heat and power for wind power integration in China: Modeling and implications, IEEE Trans. Power Syst. 30 (4) (2014) 1848–1857.
[3] A. Zlotnik, L. Roald, S. Backhaus, M. Chertkov, G. Andersson, Coordinated scheduling for interdependent electric power and natural gas infrastructures, IEEE Trans. Power Syst. 32 (1) (2017) 600–610.
[4] L. Bai, F. Li, T. Jiang, H. Jia, Robust scheduling for wind integrated energy systems considering gas pipeline and power transmission $N-1$ contingencies, IEEE Trans. Power Syst. 32 (2) (2017) 1582–1584.
[5] C. Ordoudis, P. Pinson, J.M. Morales, An integrated market for electricity and natural gas systems with stochastic power producers, Eur. J. Oper. Res. 272 (2) (2019) 642–654.
[6] C.M. Correa-Posada, P. Sánchez-Martín, Integrated power and natural gas model for energy adequacy in short-term operation, IEEE Trans. Power Syst. 30 (6) (2015) 3347–3355.
[7] A. Schwele, C. Ordoudis, J. Kazempour, P. Pinson, Coordination of power and natural gas systems: Convexification approaches for linepack modeling, Proceeding of the 13th IEEE PES PowerTech Conference, Milan, Italy, 2019.
[8] S. Chen, A.J. Conejo, R. Sioshansi, Z. Wei, Unit commitment with an enhanced natural gas-flow model, IEEE Trans. Power Syst. 34 (5) (2019) 3729–3738.
[9] C. Lin, W. Wu, B. Zhang, Y. Sun, Decentralized solution for combined heat and power dispatch through Benders decomposition, IEEE Trans. Sustain. Energy 8 (4) (2017) 1361–1372.
[10] Y. Zhou, W. Hu, Y. Min, Y. Dai, Integrated power and heat dispatch considering available reserve of combined heat and power units, IEEE Trans. Sustain. Energy 10 (3) (2019) 1300–1310.
[11] L. Mitridati, J.A. Taylor, Power systems flexibility from district heating networks, Proceeding of Power Systems Computation Conference (PSCC), Dublin, Ireland, (2018).
[12] Z. Li, W. Wu, M. Shahidehpour, J. Wang, B. Zhang, Combined heat and power dispatch considering pipeline energy storage of district heating network, IEEE Trans. Sustain. Energy 7 (1) (2015) 12–22.
[13] Y. Chen, Q. Guo, H. Sun, Z. Li, Z. Pan, W. Wu, A water mass method and its application to integrated heat and electricity dispatch considering thermal dynamics, arXiv preprint arXiv:1711.02274 (2017).
[14] M. Geidl, G. Koeppel, P. Favre-Perrod, B. Klockl, G. Andersson, K. Frohlich, Energy hubs for the future, IEEE Power Energy Mag. 5 (1) (2006) 24–30.
[15] G. Byeon, P. Van Hentenryck, Unit commitment with gas network awareness, IEEE Trans. Power Syst. 35 (2) (2020) 1327–1339.
[16] A. Belderbos, E. Delarue, W. D'haeseleer, Possible role of power-to-gas in future energy systems, Proceeding of International Conference on the European Energy Market (EEM), Lisbon, Portugal, (2015).
[17] P. Pinson, L. Mitridati, C. Ordoudis, J. Østergaard, Towards fully renewable energy systems: Experience and trends in Denmark, CSEE J. Power Energy Syst 3 (1) (2017) 26–35.
[18] L. Mitridati, P. Pinson, Optimal coupling of heat and electricity systems: astochastic hierarchical approach, Proceeding of the 16th International Conference on Probabilistic Methods Applied to Power Systems (PMAPS), Beijing, China, (2016).
[19] L. Mitridati, J. Kazempour, P. Pinson, Heat and electricity market coordination: Ascalable complementarity approach, Eur. J. Oper. Res. 283 (3) (2020) 1107–1123.
[20] G.P. McCormick, Computability of global solutions to factorable nonconvex programs: Part I – Convex underestimating problems, Math. Program. 10 (1) (1976) 147–175.
[21] M.K. Singh, V. Kekatos, Natural gas flow solvers using convex relaxation, IEEE Trans. Control Netw. Syst. (2020). To be published. https://doi.org/10.1109/TCNS.2020.2972593.
[22] C. Ordoudis, P. Pinson, J.M. Morales, M. Zugno, An updated version of the IEEE RTS 24-bus system for electricity market and power system operation studies - DTU working paper (available online), 2016, Available: http://orbit.dtu.dk/files/120568114/An.
[23] A. Schwele, A. Arrigo, C. Vervaeren, J. Kazempour, F. Vallée, Online companion: Coordination of electricity, heat, and natural gas systems accounting for network flexibility, 2020, [Online]. Available: https://doi.org/10.5281/zenodo.3463161.